

Design and Research of Active Gravity Unloading Device for Large Aperture Optical Mirror

Qiuyue Yu, Zhaoming Wang, Qiushi Yang, Wen Guo, Chunlin Li, Yonggang Wang, Mengjuan Li, Jianhua Zhang, Chao Wang

Beijing Institute of Space Mechanics & Electricity, Beijing, China

Email: 1339189033@qq.com

How to cite this paper: Yu, Q.Y., Wang, Z.M., Yang, Q.S., Guo, W., Li, C.L., Wang, Y.G., Li, M.J., Zhang, J.H. and Wang, C. (2023) Design and Research of Active Gravity Unloading Device for Large Aperture Optical Mirror. *Optics and Photonics Journal*, 13, 167-177.

<https://doi.org/10.4236/opj.2023.137015>

Received: July 4, 2023

Accepted: July 28, 2023

Published: July 31, 2023

Abstract

The large aperture optical mirror for space is processed and tested in the gravity environment on the ground. After entering space, gravity disappears due to the change of environment, and the mirror surface that has met the engineering requirements on the ground will change, seriously affecting the imaging quality. In order to eliminate the influence of gravity and to ensure the consistency of space and ground, gravity unloading must be performed. In order to meet the requirements of processing and testing for the large aperture space mirror in the state of vertical optical axis, a universal gravity unloading device was proposed. It was an active support and used air cylinders to provide accurate unloading force. First, the design flow of gravity unloading was introduced; then the detailed design of the mechanical structure and control system was given; then the performance parameters of the two types of cylinders were tested and compared, including the force-pressure relationship curve and the force-position relationship curve; finally, the experimental verification of the gravity unloading device was carried out; for a mirror with an aperture of $\varnothing 2100$ mm, the gravity unloading device was designed and a vertical detection optical path was built. The test results showed that by using this gravity unloading device, the actual processing surface accuracy of the mirror was better than $1/50\lambda$ -RMS, which met the application requirement of the optical system. Thus, it can be seen that using this gravity unloading device can effectively unload the gravity of the mirror and realize the accurate processing and measurement of the mirror surface.

Keywords

Optical Mirror, Large Aperture, Active Support, Gravity Unloading

1. Introduction

With the continuous development of remote sensing technology, in order to meet the requirements of large field of view, wide coverage and high resolution of the optical system [1] [2] [3] [4], the aperture of the optical mirror has become larger and larger, and the requirements of surface shape accuracy have also become higher and higher, which makes the processing and detection of the mirror more difficult. Since the optical mirror is processed and tested in the gravity environment on the ground, after entering space, the gravity will disappear due to the change of environment, and the mirror surface shape will change, which will seriously affect the imaging quality of the mirror [5]. In order to effectively unload gravity, eliminate the influence of gravity and ensure the consistency of heaven and earth, the gravity unloading device is used in the mirror shape detection process. According to whether the supporting force can be actively adjusted, the gravity unload device can be divided into two types of active support and passive support [6] [7] [8]. The support force of active support can be controlled and adjusted with high support accuracy, but its support structure may be more complex. The support force of passive support cannot be adjusted and the support accuracy is low, but the distribution of support points is easy to calculate and the structure is simple. From the current research status of large aperture space mirror support technology at home and abroad, it can be seen that in order to achieve high precision gravity unloading of large aperture mirrors, active support has been widely studied [9] [10].

At present, the active gravity unloading device mostly uses the force actuator structure [11] [12]. The specific form is to arrange several force actuators on the back of the mirror, and use the force exerted by the actuators to compensate for gravity. In essence, this method is to apply an upward force field to the back of the mirror so that the resultant force of the mirror in a gravity environment is 0 N, thereby indirectly simulating the state of weightlessness. For example, the Hubble Space Telescope (HST) adopted 134 active support points during ground processing. By accurately calculating the support force of each support point, the emulation of the zero-gravity state under the vertical optical axis was realized, and the processing accuracy of the reflective mirror shape within the range of 2.4 m aperture was 6.4 nm RMS [13]. The Supernova Acceleration Probe (SNAP) was a new-generation telescope in the United States. Its aperture was 2050 mm, and the RMS surface shape accuracy in orbit was required to be better than 10 nm. During the ground processing and detection process, 57 active support points were used, and the RMS of the surface shape processing accuracy was ultimately better than 6.8 nm [14].

Aiming at the detection requirement of the optical axis vertical state of the space large aperture mirror, this paper proposes an active gravity unloading support device, which is universal and uses the cylinder to provide the support force, and gives the detailed design of the mechanical structure and control system. Finally, the experimental verification of the device was carried out. Using

this gravity unloading support device, the actual surface shape accuracy RMS of the mirror was better than $1/50\lambda$. The experimental results show that the device can effectively unload gravity and realize high precision processing and detection of the mirror.

2. Theoretical Design

2.1. Design Flow

The active gravity unloading device is mainly designed for the meter caliber mirror, and the cylinder is selected to support the force, this device can meet the plane, spherical and aspherical mirror processing and detection. **Figure 1** shows the specific design flow of the gravity unloading device. For a mirror, the first step is to carry out gravity unloading simulation analysis, so as to determine the number of unloading points, the size of the force value and the specific distribution. Then, taking into account the feasibility of the project implementation, all points with similar force value are combined into one gas circuit. As the force is provided by the cylinder, it is necessary to calibrate the cylinder one by one due to the difference in cylinder performance. The cylinders with similar performance parameters are grouped in the same gas circuit to ensure that the support force provided by each cylinder in the circuit is as same as possible under the same air pressure. Then the mechanical structure is designed, and finally the control system is designed.

2.2. Detailed System Design

The gravity unloading device is divided into two parts: the mechanical system and the control system. The mechanical system refers to the mechanical structure of the gravity unloading device. **Figure 2** shows a three-dimensional model of the mechanical structure, which is mainly consists of the base plate, air cylinder, support plate, support column, positioning guide column, tangential position limiter and displacement sensor. The base plate supports the entire structural system and must ensure a certain degree of rigidity. Moreover, the cylinder is connected to the base plate by bolts, so the base plate is an important part to define the position of the cylinder. According to the processing conditions, the position error of the cylinder connecting hole on the base plate can be controlled within 0.1 mm. The cylinder is the realization unit of the force actuator, placed at the correct support point position, by providing accurate force to support the mirror, the cylinder push rod is connected with extension rod and ball cap, the ball cap is attached with 3 M rubber pad to achieve soft contact and prevent bumping the mirror. The support plate, before the force of the cylinder is applied to the mirror, the mirror is placed on the support plate, and the support plate

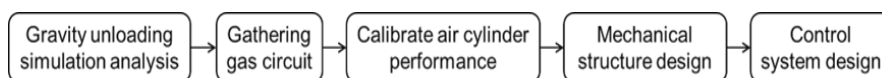


Figure 1. The design flow of gravity unloading device.

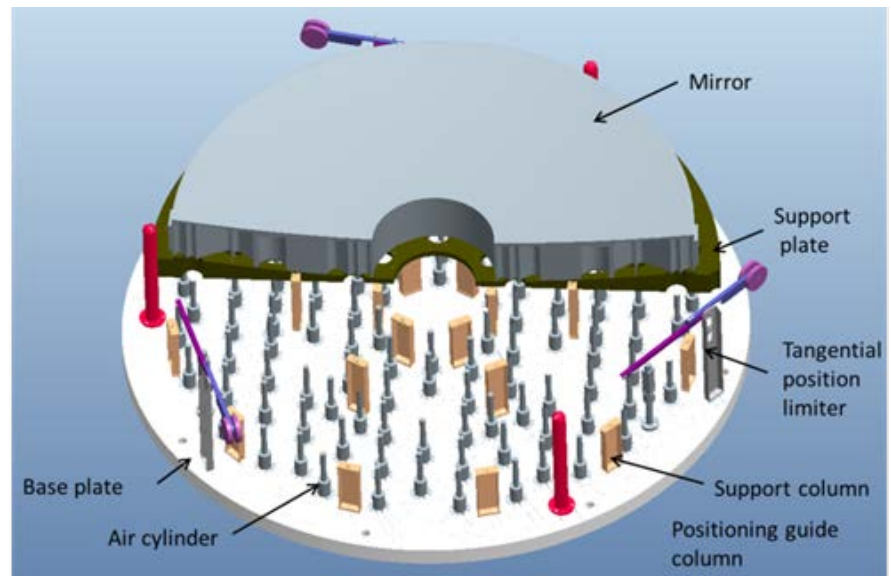


Figure 2. Three-dimensional model of the mechanical structure.

has corresponding holes according to the position of the support point, when the cylinder is supplied with air, the push rod of the cylinder rises up, and the top ball cap can contact the back of the mirror through the holes, thus supporting the mirror from the support plate to achieve gravity unloading. The connection between the support and the base plate is realized by the support column. The positioning guide column is arranged on the base plate to play the role of positioning guide, and it is evenly distributed at 120° to ensure that the gravity unloading device has good repeat positioning ability. The tangential position limiter is evenly distributed on the base plate at 120° , its function is to limit the horizontal movement of the mirror and play the role of side protection. The displacement sensor is also evenly distributed at 120° and touches the back edge of the mirror to provide real-time feedback on how high the mirror is lifted and whether the mirror is tilted during gravity unloading.

The air cylinder, support column, positioning guide column, tangential position limiter and displacement sensor in the mechanical structure of the gravity unloading device are universal for all mirrors of different calibers, only the base plate and support plate need to be designed according to the corresponding mirror. According to the structure size of the mirror and the simulation analysis of gravity unloading, the connecting holes and the specific structure shape of the base plate and the support plate are designed.

The control system mainly consists of computer (PC) with control interface, programmable logic control system (PLC) and solenoid valve and other components. **Figure 3** shows the block diagram of the control system, the type of solenoid valve controlling each gas circuit is Type 6011, which has a fast execution speed and the shortest cycle time is 20 ms. To achieve high efficiency and high precision of gas supply, two different flow rates of gas supply are provided by proportional valves, which are high flow and low flow. When the air pressure is

far from the set value, it is a high flow supply, and when it is close, it becomes a low flow, thereby improving the efficiency of the gas supply. The specific control principle is through the computer input command to the PLC, the PLC controls the corresponding proportional valve and solenoid valve, and then achieve the control of air pressure in each circuit cylinder. In the whole operation process, the pressure sensor real-time monitoring and feedback the gas pressure value in the gas circuit, the position sensor can real-time feedback the height of the mirror and whether the mirror tilts.

Figure 4 shows the physical picture of the control system. At present, the control system can simultaneously control the air pressure supply of 36 gas circuits.

3. Cylinder Performance Calibration Test

Before assembling and commissioning of the gravity unloading device, it is necessary to calibrate each cylinder, test the relationship between the force and the air pressure of the cylinder, and the relationship between the force and the position of the cylinder, cylinders with similar parameters are placed in the same gas

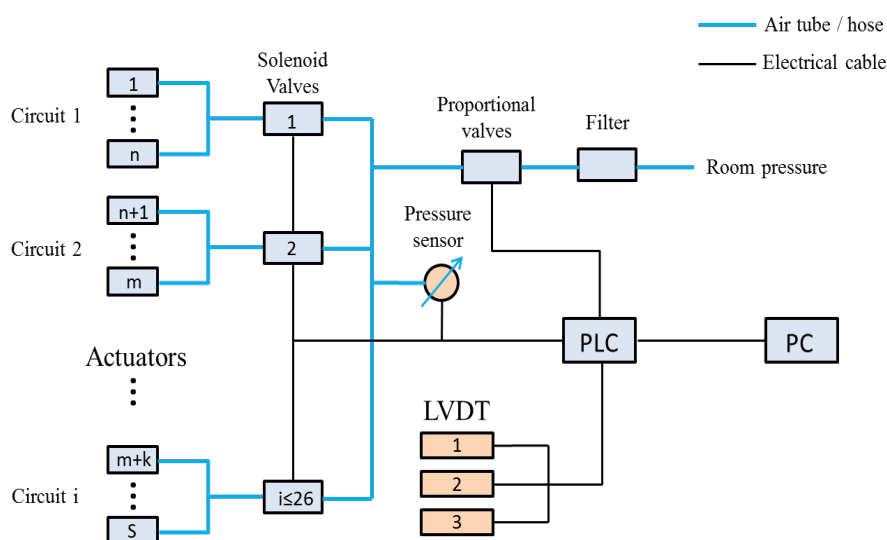


Figure 3. The logic diagram of control system.

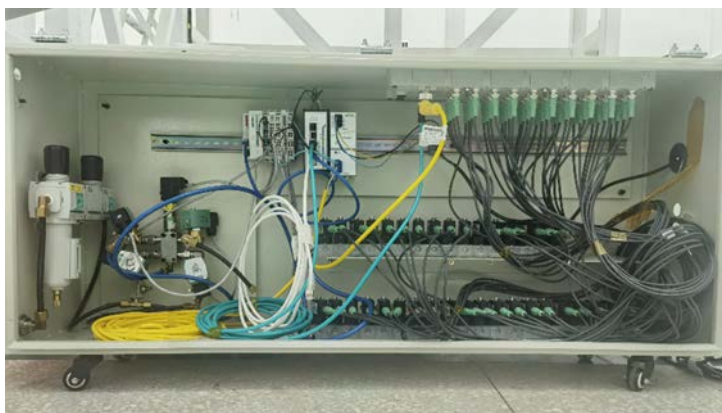


Figure 4. The physical picture of control system.

circuit and the parameters of the cylinder in the same gas circuit are entered into the software program as a configuration file. The force-pressure curves and force-position curves of a French brand air cylinder and a Japanese brand air cylinder were tested here.

Figure 5 gives the relationship curve between force and pressure for the French cylinder, with the test position selected as cylinder midstroke of the cylinder (0 mm), midstroke +0.5 mm and midstroke -0.5 mm. As can be seen from the figure, the cylinder had a high degree of linearity and the support force provided in the pressure test range was approximately between 7 N and 86 N, and the maximum absolute error was 0.7 N.

Figure 6 shows the relationship curve between force and position in the France cylinder with the air pressure selected as 50 mbar, 250 mbar and 450 mbar respectively. The lower the slope of the force-position curve, the better the stiffness of the cylinder, and the most ideal state is that the slope is equal to 0. As can be seen from **Figure 6**, the actuator had a good stiffness and the maximum absolute error was 0.9 N within ± 0.5 mm of the the cylinder midstroke.

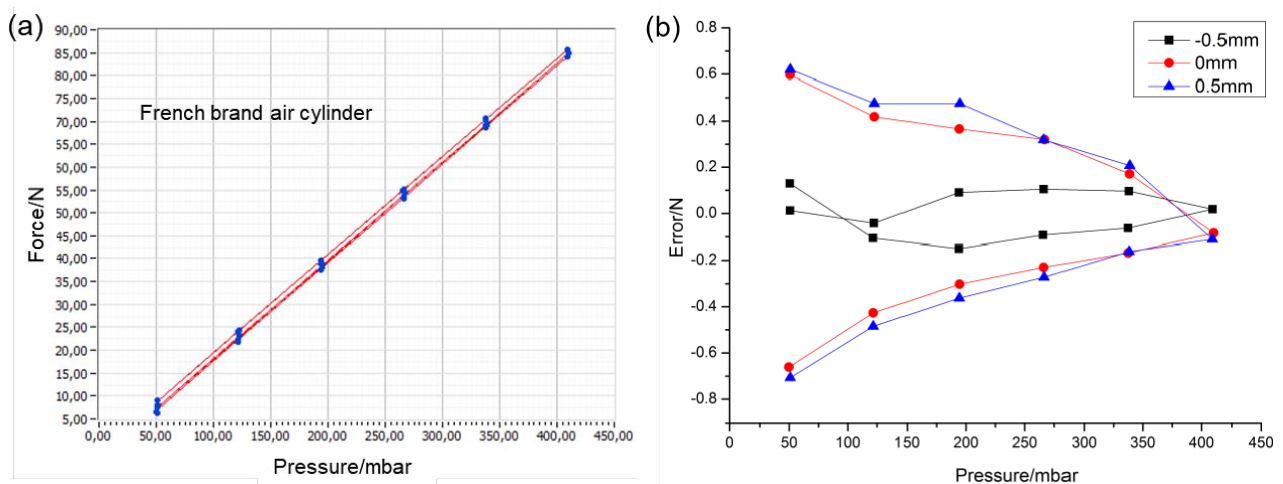


Figure 5. (a) The relation curve between force and pressure of French brand air cylinder; (b) The corresponding error curve.

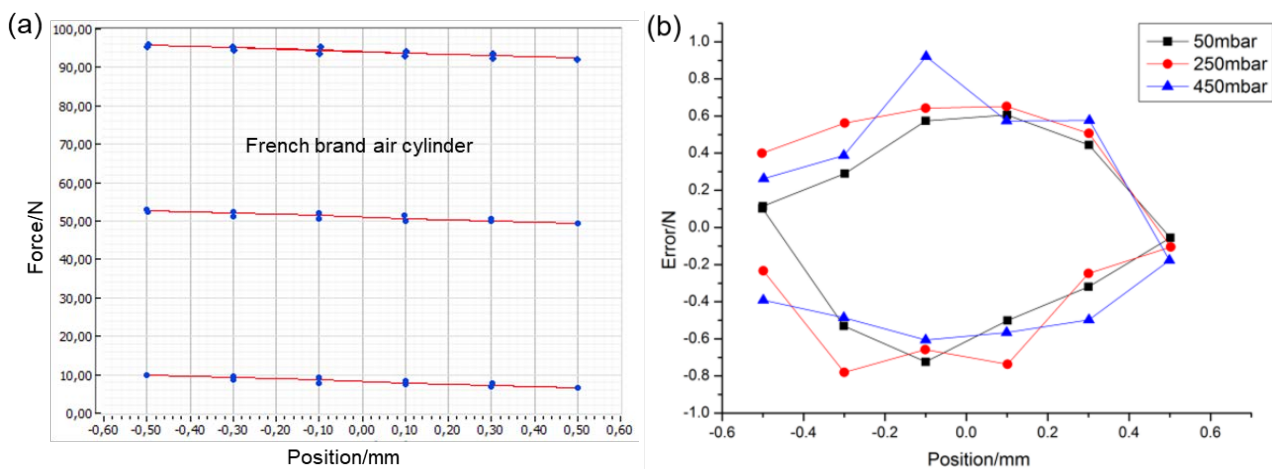


Figure 6. (a) The relation curve between force and position of French brand air cylinder; (b) The corresponding error curve.

Figure 7 shows the relationship curve between force and pressure for the Japanese cylinder, with the test position selected as the midstroke of the cylinder (0 mm), midstroke +0.5 mm and midstroke -0.5 mm. As can be seen from the relationship curve, the linearity of the cylinder was very good, and it was less affected by the position. In the pressure test range, the force provided by the cylinder was approximately 2.5 - 47.5 N, and the maximum absolute error was 0.175 N.

Figure 8 shows the relationship curve between force and position in the Japanese cylinder with the air pressure selected as 50 mbar, 250 mbar and 450 mbar respectively. As can be seen from the relationship curve, the actuator had a good stiffness and the maximum absolute error was 0.35 N within ± 0.5 mm of the cylinder midstroke.

Based on the results of the performance calibration test, the comparison of the performance parameters of the two types of air cylinders is shown in **Table 1**. According to the test results, both the French cylinder and the Japanese cylinder had high linearity, but under the same air pressure, the force range of the two

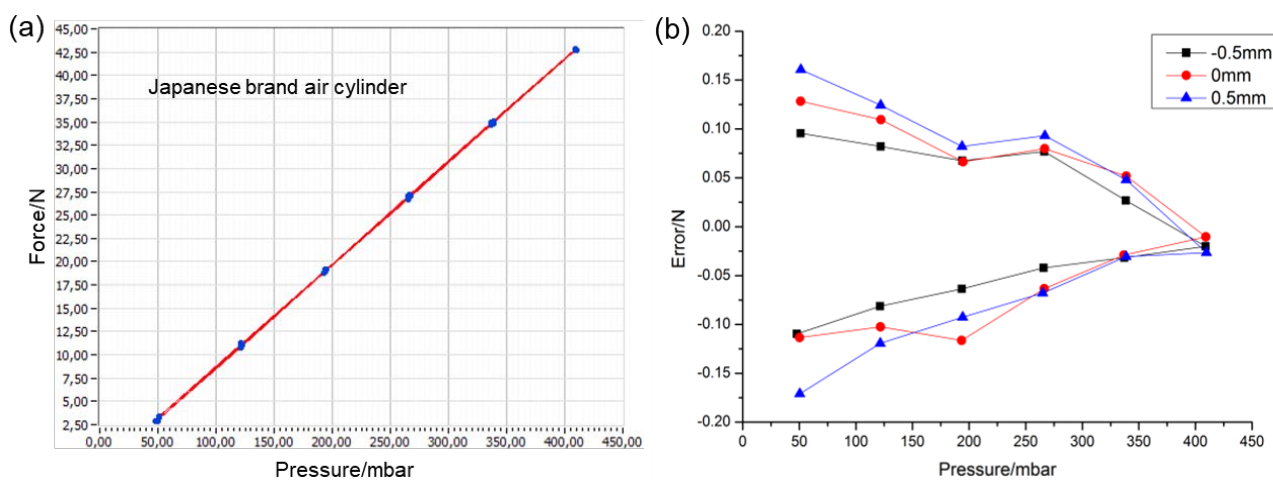


Figure 7. (a) The relation curve between force and pressure of Japanese brand air cylinder; (b) The corresponding error curve.

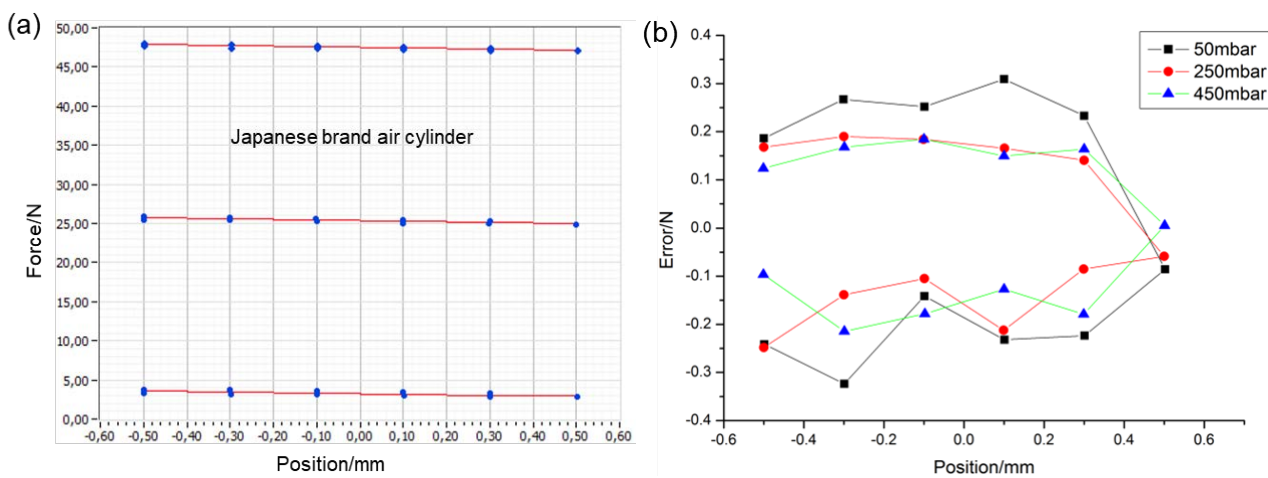


Figure 8. (a) The relation curve between force and position of Japanese brand air cylinder; (b) The corresponding error curve.

cylinders was different. The French cylinder provided a wide force range, but it was not sensitive to small forces and cannot be used for testing below 10 N, and its error accuracy was not as good as that of the Japanese cylinder. While the force range provided by the Japanese cylinder was relatively small under the same air pressure. Since the change of cylinder type does not affect the control system, in actual operation the French cylinder and the Japanese cylinder were mixed, the French cylinder was used at the support point of the large force, and the Japanese cylinder was used at the support point of the small force, which could reduce the cost and improve the accuracy. However, it should be noted that the cylinders cannot be mixed in the same gas circuit.

4. Experiment and Result

The gravity unloading device was designed for a specific $\text{Ø}2100$ mm aperture mirror. According to the number of support points, the force value and the specific distribution position calculated by simulation, the corresponding cylinders were selected and the base plate and support plate were designed in detail. Other components of the gravity unloading structure and the control system were universal and only needed to be assembled as required. The physical picture of the designed gravity unloading device is shown in **Figure 9**.

The detection optical path was built, and the interferometer and compensator were selected for detection. Under the vertical state of optical axis, the test state is shown in **Figure 10**.

During the test, the coaxial mirror can generally remove certain system errors by the rotation method. The implementation was to keep the interferometer, compensator and gravity unloading device fixed, rotate the mirror and obtain

Table 1. Comparison of performance parameters of two types of air cylinder.

	French brand air cylinder	Japanese brand air cylinder
Force range	7 - 86 N	2.5 - 47.5 N
Error accuracy	± 0.9 N	± 0.35 N



Figure 9. The physical picture of gravity unloading device.

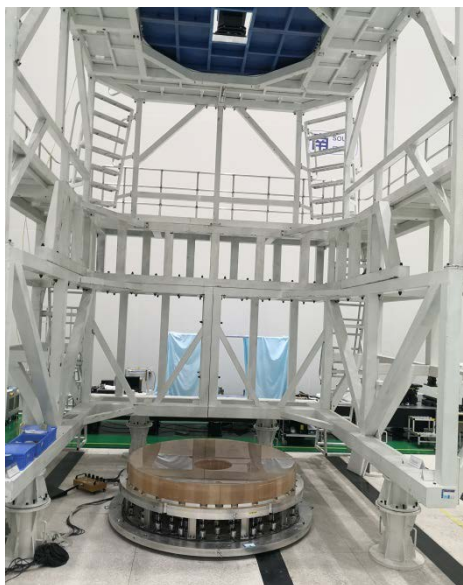


Figure 10. The picture of test site.

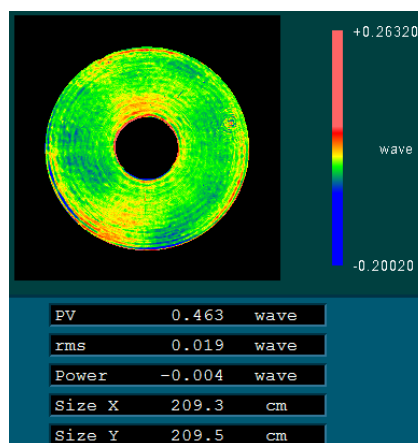


Figure 11. The surface shape detection result under vertical optical axis.

the test surface shape in three directions of 0° , 120° and 240° . The surface shape data in these three directions were processed and the test results after removing the system errors are shown in **Figure 11**. It can be seen that the surface shape accuracy of the mirror was better than $1/50\lambda$ -RMS, which met the requirements of the optical system.

5. Conclusion

In order to meet the detection requirement of the space large aperture optical mirror in the state of vertical optical axis, this paper presents a universal type active gravity unloading device which uses cylinder to provide supporting force. First, the design flow of the gravity unloading device was introduced. Then, the mechanical structure and control system were designed in detail, and the performance parameters of the two cylinders were tested and compared, including the force-pressure relationship curve and the force-position relationship curve.

Finally, the experimental verification of the gravity unloading device was carried out, and for a specific $\varnothing 2100$ mm aperture mirror, the gravity unloading device was designed and the detection optical path was built. The test results showed that the actual machining surface accuracy RMS of the mirror was better than $1/50\lambda$ by using the gravity unloading device, which met the requirements of the optical system. It can be seen that by using the gravity unloading device, gravity can be effectively unloaded and high-precision mirror surface shape processing can be achieved.

Conflicts of Interest

The authors declare no conflicts of interest regarding the publication of this paper.

References

- [1] Kendrick, S.E. and Stahk, H.P. (2008) Large Aperture Space Telescope Mirror Fabrication Trades. *SPIE*, **7010**, 70102G. <https://doi.org/10.1117/12.788067>
- [2] Wang, Y.G., Li, A., Meng, X.H., Li, W.Q. and Zhang, J.Y. (2021) Thermal Effect in Ion Beam Figuring of Optical Mirror Assembly. *Spacecraft Recovery & Remote Sensing*, **42**, 72-78.
- [3] Yang, Q.S., Zhang, J.Y., Yu, J.H., Chen, J.C. and Yu, Q.Y. (2020) Research on Error Analysis of Support Deformation for Large Aperture Space Mirrors. *Spacecraft Recovery & Remote Sensing*, **41**, 60-70.
- [4] Cao, H.Y., Zhang, X.W., Zhao, C.G., Xu, C., Mo, F. and Dai, J. (2020) System Design and Key Technologies of the Satellite. *Chinese Space Science and Technology*, **40**, 1-9. <https://doi.org/10.11728/cjss2020.04.578>
- [5] Wang, X.Y. (2018) Development and Prospect of Space Optical Technology. *Spacecraft Recovery & Remote Sensing*, **39**, 79-86.
- [6] Cavaller, L., Marrero, J., Castro, J., Morante, E., Ronquillo, M. and Hernandez, E. (2008) Design of the Primary Mirror Segment Support System for the E-ELT. *Society of Photo-Optical Instrumentation Engineers (SPIE) Conference Series*, 70121F-11. <https://doi.org/10.1117/12.789784>
- [7] Janssen, H., Geurink, R., Teuwen, M. and Bree, B.V. (2008) Development of a Novel Actuator Concept for Position Control of Segmented Mirrors of ELT. *Proc SPIE*, **6267**, 70123F-7. <https://doi.org/10.1117/12.787914>
- [8] Shao, L., Wu, X.X., Yang, F., Fan, L. and Li, J.F. (2014) Improvement on Hydraulic Whiffletree Support System for SiC Lightweight Primary Mirror. *Infrared and Laser Engineering*, **43**, 3820-3824.
- [9] Neufeld, C., Zolcinski-Couet, M.C., Keane, M. and Ruthven, G. (2004) The Primary Mirror System for the SOAR Telescope. *SPIE*, **5489**, 870-880. <https://doi.org/10.1117/12.551375>
- [10] Wu, X.X., Li, J.F., Song, S.M., Shao, L. and Ming, M. (2014) Active Support System for 4 m SiC light Weight Primary Mirror. *Optics and Precision Engineering*, **22**, 2451-2457. <https://doi.org/10.3788/OPE.20142209.2451>
- [11] Fan, L., Wang, Z. and Cao, Y.Y. (2015) Analysis of Mirror Support Based on Active Moment Correction. *Infrared and Laser Engineering*, **44**, 1273-1277.
- [12] Li, J.F., Wu, X.X. and Shao, L. (2016) Study on Active Support for Large SiC Prima-

-
- ry Mirror and Force Actual or Design. *Infrared and Laser Engineering*, **45**, 1-5. <https://doi.org/10.3788/irla201645.0718003>
- [13] Montagnino, L.A. (1985) Test and Evaluation of the Hubble Space Telescope 2.4-Meter Primary Mirror. *Proceedings of SPIE*, **571**, 182-190. <https://doi.org/10.1117/12.950408>
- [14] Schubnell, M., Dorn, D.A., Holland, A.D., Barron, N., Bebek, C., Borysow, M., Brown, M.G., Cole, D., Figer, D. and Lorenzon, W. (2006) Near Infrared Detectors for SNAP. *Proc. of SPIE*, **6276**, 1-4. <https://doi.org/10.1117/12.672436>